NASA Technical Memorandum 81489

SIMULATION OF TRANSDUCER-COUPLANT EFFECTS ON BROADBAND ULTRASONIC SIGNALS

Alex Vary
Lewis Research Center
Cleveland, Ohio

Prepared for the
Spring Meeting of the American Society for Nondestructive Testing
Philadelphia, Pennsylvania, March 24-27, 1980

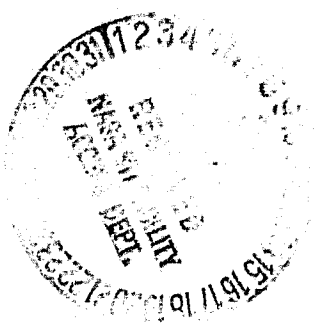

SIMULATION OF TRANSDUCER-COUPLANT EFFECTS ON BROADBAND ULTRASONIC SIGNALS

Alex Vary

National Aeronautics and Space Administration
Lewis Research Center
Cleveland, Ohio 44135

ABSTRACT

The increasing use of broadband, pulse-echo ultrasonics in nondestructive evaluation of flaws and material properties has generated a need for improved understanding of the way signals are modified by coupled and bonded thin-layer interfaces associated with transducers. This understanding is most important when using frequency spectrum analyses for characterizing material properties. In this type of application, signals emanating from material specimens can be strongly influenced by couplant and bond-layers in the acoustic path. Computer sythesized waveforms were used to simulate a range of interface conditions encountered in ultrasonic transducer systems operating in the 20- to 80-MHz regime. The adverse effects of thin-layer multiple reflections associated with various acoustic impedance conditions are demonstrated. The information presented is relevant to ultrasonic transducer design, specimen preparation, and couplant selection.

E-427

INTRODUCTION

Ultrasonics for flaw detection and materials characterization is a significant area in nondestructive evaluation (NDE) technology (refs. 1-5). The methodology usually involves broadband transducers in contact with surfaces of test specimens. When frequency spectrum analysis is used for characterizing flaws and material properties, the results can be strongly influenced by couplant and bond-layers associated with the transducer (ref. 1). These thin bond layers and also interconnecting cables can significantly alter the frequency spectra of high-frequency, broadband signals such as those used in making ultrasonic attenuation measurements (refs. 2, 4, 5). For example, spectrum distortions can arise from interference effects due to multiple reflections in thin bond layers. In the case of couplant layers the magnitude of the pressure applied to the ultrasonic probe determines the resultant couplant thickness. Couplant thickness is an important factor in determining the character and acceptability of the signals from a material (refs. 1, 5, 6). The magnitude and nature of signal distortions caused by bond-layer and couplant thickness variations and their related acoustic impedance effects are oftentimes ignored and inadequately understood.

This report treats the effects of thin couplant and bond-layers associated with transducers. Computer simulation methods are used to illustrate the way signals emanating from material specimens can be distorted by thin layers in the acoustic path. Examples are given to demonstrate the adverse effects of thin layers and also coaxial cables. In addition, conditions

under which satisfactory results can be obtained are presented. This paper is believed to be the first attempt to give a systematic account of thin-layer effects as a function of layer thickness and acoustic impedance relative to adjacent materials. The information presented herein is relevant to broadband transducer construction, specimen preparation, and couplant and bond selection and can be an aid in recognizing unacceptable waveforms arising from signal distortions.

APPROACH

The key parameters examined are couplant and bond-layer thickness variations and acoustic impedances of materials commonly occurring in contact ultrasonic involving broadband, buffered probes (refs. 2-5). The frequency range considered is from approximately 20 to 80 MHz, centered at 50 MHz. This range is important in the ultrasonic characterization of the mechanical properties of a variety of materials. It is also a range in which the adverse effects of thin layers become significant. The associated layer thickness are from zero to 50 μm which correspond to the wavelengths involved.

The experimental difficulty of actually varying layer thickness at uniformly spaced intervals from 0 to 50 μm for a number of material combinations is avoided by use of a computer simulation technique. Using this approach, mathematically synthesized waveforms are analyzed by means of a high-speed digital computer and array processing algorithms. The physical acoustics are straightforward, based on the premise of plane elastic waves. The results can be shown to be in excellent agreement with effects that can be observed by direct experimentation, as discussed later.

The transducer-specimen configuration illustrated in figure 1 is taken as a model (refs. 7, 8). As indicated in the figure, the principal material components are an absorber, a piezoelectric element, a buffer, bond layers, a couplant, and the test specimen. The analysis is restricted to consideration of a broadband, ultrasonic pulse signal moving from the specimen into the piezoelement and thence into the adsorber. The buffer serves primarily as a delay line that isolates the piezoelement and specimen. The purpose of the adsorber is to prevent reentry of signals into the piezoelement.

Although the analysis herein treats acoustical reverberations in thin layers, the results are analogous to electronic reflections in coaxial cables used to couple the transducer to a receiver network, as discussed later. In all cases herein, the actual ultrasonic waves in the materials are depicted and referred to in terms of their electrical signal analogs, such as those emitted by the piezoelement in response to a transient pressure wave.

GOVERNING EQUATIONS

A series of configurations, each involving three materials, are treated in accordance with the schedule given in table 1. In each case, the central material is the thin layer of bond or couplant. Transmission of ultrasonic signals through the thin layer is analyzed by using the conventions illustrated schematically in figure 2. As shown in the figure, signal progression is from material [3] through [2] into [1]. (The wave vectors are normal to the interfaces, not oblique as shown for schematic purposes.)

In general, the acoustic impedances of the three materials will differ and hence give rise to the indicated multiple reflections within the thin layer. The signal, E, that emerges in material [1] will tend to be an unresolved composite formed by superposition of the successive thin-layer reflections E_0 through E_N. Once formed, E is unresolvable into its components unless the layer thickness exceeds the mean wavelength of the source signal, S. The spectrum of E will differ from that of S by varying degrees depending on layer thickness, acoustic impedances, and attenuation in the layer.

The transmission, T, and reflection, R, coefficients for the interfaces [1] - [2] and [2] - [3] are given in terms of the acoustic impedances, Z, with dual subscripts indicating direction (ref. 9).

$$T_{21} = \frac{2Z_1}{Z_2 + Z_1}, \quad T_{12} = \frac{2Z_2}{Z_2 + Z_1} \tag{1}$$

$$T_{32} = \frac{2Z_2}{Z_3 + Z_2}, \quad T_{23} = \frac{2Z_3}{Z_3 + Z_2} \tag{2}$$

$$R_{12} = -R_{21} = \frac{Z_2 - Z_1}{Z_2 + Z_1} \tag{3}$$

$$R_{23} = -R_{32} = \frac{Z_3 - Z_2}{Z_3 + Z_2} \tag{4}$$

The amplitudes of the successive reverberation signals E_0 to E_N are determined by tramission and reflection coefficients and layer thickness, t, and attenuation coefficient, A:

$$\begin{aligned} E_0 &= ST_{32}T_{21} \exp(-At) \\ E_1 &= E_0R_{21}R_{23} \exp(-2At) \\ E_2 &= E_0R_{21}^2R_{23}^2 \exp(-4At) \\ E_N &= E_0R_{21}^NR_{23}^N \exp(-2NAt) \end{aligned} \tag{5}$$

Each successive signal lags the preceding one by the layer "round trip" delay time, d, where $d = 2t/v$, and v is the velocity in the layer. The composite signal E is formed by summing time-domain amplitude waveforms, each displaced by the parenthetically indicated delay:

$$E = E_0 + E_1(-d) + E_2(-2d) + \ldots + E_N(-Nd) \tag{6}$$

This type of summation is readily accomplished by computer processing of waveform arrays.

In the special case where the acoustic impedance of the layer equals or closely approximates that of one contiguous material (i.e., $Z_2 \cong Z_3$ or $Z_2 \cong Z_1$),

$$E = SI_{31} \exp(-At) \qquad (7)$$

where $T_{31} = 2Z_1/(Z_3 + Z_1)$. As layer thickness approaches zero, $E \rightarrow SI_{31}$.

WAVEFORM SYNTHESIS

The starting waveform, S, is synthesized from ideal amplitude and phase spectra. The procedure is illustrated in figure 3. To assure that the synthesized waveform is authentic, an actual signal is acquired, digitized, and analyzed in polar form by Fourier transformation. By using the real waveform as a model, classical Gaussian amplitude and linear phase spectra are created. Inverse Fourier transformation is used to synthesized a source waveform, S. This procedure assures that any subsequent distortions become evident upon inspection of the composite waveform, E. The synthetic waveform, S, is normalized to 1 volt (minimum to maximum) and thereafter used as a standard source signal for a particular center frequency and bandwidth.

Computer processing of S proceeds with the creation of waveform arrays for E_0 through E_N in accordance with the preceding equations. Economization of computer time requires selection of the smallest permissible number, N, of thin-layer reflections consistent with simulation of actual conditions. Selection of $N = 10$ is satisfactory for the range of materials and conditions investigated herein. This follows from the fact that the amplitude of each successive reflection is diminished exponentially according to the attenuation coefficient of the layer material.

The output composite waveform, E, is synthesized by array addition of corresponding time-domain elements of E_0 through E_N. This corresponds to matrix addition of amplitudes of the N pressure wave components. The composite waveform, E, is subsequently Fourier transformed into polar amplitude and phase spectra and the results are exhibited graphically, as explained in the next section.

RESULTS

The results presented are restricted to a few key material combinations that illustrate pivotal conditions. These materials and acoustical properties are listed in table II. The graphical results and associated data are organized and presented in the order indicated in table I, in seven sets of figures, figures 4 to 10. The first figure in each set summarizes the data associated with the remaining figures. The remaining figures in each set appear in order of increasing layer thickness and show variations in the composite waveform, E, and its amplitude spectrum as layer thickness increases from zero to 40 μm. For all the material combinations examined, the phase spectra remain linear, with no significant change in slope, and exhibit no interesting features with increasing layer thickness. Phase spectra are therefore omitted.

In figures 4 to 10, the OUT/IN amplitude gives the current value of the ratio E/S for each thickness. The RMS (root mean square) energy level is the ratio of the current energy of E relative to its initial value at zero thickness. The variation of the RMS energy level with layer thickness is shown in the summary graphs at the beginning of each set of figures. Spec-

tral skewing is a measure of signal distortion and is computed as percent displacement of the current peak frequency from the nominal (i.e., original) peak frequency associated with the undistorted waveform at zero thickness. The dashed curve in the amplitude spectrum graph is included to show the amount of spectrum distortion that accompanies increasing layer thicknesses.

DISCUSSION

For material combinations having poorly matched acoustic impedances, the least energy transfer (i.e., minimum RMS energy for the composite signal E) occurs at layer thicknesses of 1/4 wavelength (figs. 4(a), 7(a), and 9(a)). Under this condition destructive interference prevails. A secondary maximum follows at layer thicknesses of 1/2 wavelength because of constructive interference. The relative normalized RMS energy levels of these minima and maxima are identical irrespective of the source-signal center frequency. For example, at 20 MHz center frequency, RMS curves are similar to those in figure 4(a) except that they "stretch" to the right, i.e., the 1/4 wavelength minima occur further to the right and initial negative slopes are less.

The adverse effects of multiple reflections in thin layers become apparent by comparing amplitude spectra shown in figures 4, 7, and 9 for 1/2 wavelength layers. For example, figures 4(h), 7(i), and 9(i) illustrate a classical reduction in spectral bandwidth as the result of a "ringing" layer. These figures contrast sharply with the virtually undisturbed broadband spectra obtained with impedance matching (figs. 5, 6, 8, and 10, e.g.). Figures 4, 7, and 9 also illustrate that although RMS energy reduction with increasing layer thickness may appear tolerable, the associated spectral distortions can be quite unacceptable. Certainly, any procedure that relies on spectrum analysis must at least take account of such distortions and avoid them, if possible.

When different materials are combined, there are practical limitations on the ability to control acoustic impedances. By way of compromise, an alternative to perfectly matched impedances would simply require, for example, that

$$Z_1 \leq Z_2 < Z_3 \quad \text{or} \quad Z_1 > Z_2 \geq Z_3$$

wherein the layer acoustic impedance lies between that of contiguous materials; see figures 5, 6, 8, and 10. In these cases, there is a much smaller loss of signal strength due to reverberations: the RMS level of E drops by less than 5 percent as compared with ~50 percent (fig. 5(a) vs. fig. 4(a)) as layer thickness approaches 1/2 wavelength. Moreover, inteference effects become insignificant relative to attenuation, as predicted by the previous equation for $Z_2 \cong Z_1$ or $Z_2 \cong Z_3$, equation (7). Energy loss due solely to attenuation is indicated by the dashed lines in the first graph of each set (figs. 4 to 10). Examination of figures 5(a), 6(a), 8(a), and 10(a) indicates that for layers with intermediate impedances the composite signal will have only slight or no distortion because it is merely diminished by attenuation in the layer.

Close attention to coupling conditions in contact ultrasonics has been urged by previous investigators (refs. 1, 5, 6). Optimum coupling demands virtually perfect flatness for the buffer-specimen interface and the appli-

cation of substantial force to minimize the couplant layer. Figure 4 shows that in the 20- to 80-MHz range couplant thickness should be less than approximately 1 μm to avoid serious spectral distortions in the case of the typical materials: fused quartz, glycerine, and steel. This requirement is primarily a result of the acoustic mismatch of the glycerine with the contiguous materials. Among the practical alternatives to glycerine that are convenient and safe to use (water, oils, gels, silicones), none have acoustic impedances that are significantly different.

It is apparent in figure 5 that an ideal fluid couplant, fluid-X, would have an acoustic impedance close to that of the buffer material (e.g., glass or quartz). It would allow free movement of the transducer over the specimen surface and would relax surface flatness tolerances. Fluid-X also allows the couplant-layer thickness to exceed 10 μm without serious consequences on signal fidelity. Methylene iodide would qualify as fluid-X with an acrylic buffer; see figure 6. In cases where the very low attenuation and ruggedness of fused quartz are preferred, potential candidates for fluid-X are colloidal suspensions of submicrometer particles of metal, metal oxides, or ceramics. Gallium may be useful in restricted applications since it liquefies at ~30° C and readily wets glasses.

The effect of couplant thickness variations shown for synthetic waveforms in figures 4(b) to (l) can be readily verified by applying increasing force to a specimen held against a similar buffered transducer. The source signal can be the first echo from the free back surface of the specimen. As the pressure is increased and the couplant thickness diminishes, a sequence of waveforms on an oscilloscope will duplicate those appearing in the figures. If the buffer and specimen surfaces are sufficiently flat, and the couplant thickness is uniform to within 1 μm, an essentially undistorted waveform will be observed, if the transducer itself is free of internal distorting layers.

As indicated in figures 8 and 10, bond-layers (within the transducer) with intermediate impedances yield good signals over a thickness range of approximately 40 μm. These examples assume that the absorber and bond both consist of tungsten-loaded epoxy. The ideal situation would be to cast and cure the absorber material in place and thus avoid the bond-layer altogether. However, better properties are achieved if the absorber material is formed separately under high-pressure curing (ref. 7). The previous reference also suggests tailoring tungsten-loaded epoxy bond-layers that approach the acoustic impedance of PZT piezoelements (see table II). To satisfy broadband damping conditions, the bond-layer on either side of the piezoelement should have either slightly higher or slightly lower acoustic impedance (ref. 9). The results presented herein suggest that the bond-layer thickness is not critical under this condition, and therefore, it does not need to be held to a few micrometers.

It can usually be assumed that the ultrasonic receiver, oscilloscope, and associated electronic networks amplify and reproduce signals emitted by the piezoelement in a consistent-manner. However, the coaxial cable that links the transducer to the electronic network can introduce severe distortions in the signal. In this case, the cable is analogous to a thin layer sustaining multiple reflections. Resultant waveform distortions can be shown to be identical to those appearing in figures 4, 7, and 9 as a result of thin-layer reverberations. For coaxial cables having lengths of approximately 1 m, delay times are in excess of 3 nsec, and they are of the same order as delays in thin layers several micrometers thick.

To assure undistorted signal transmission, there should be electrical impedance matching of the cable to both the transducer and electronic network. The impedance of the cable should match the 50-ohm terminations conventionally provided in ultrasonic systems. Nevertheless, additional fine adjustment may be required and can be provided by adding variable resistors at either end of the cable, as illustrated in figure 11. A "damping' resistor for this purpose is usually shunted across the cable input connector in ultrasonic receivers. A variable, auxiliary damping resistor built into the transducer housing, as in figure 11, greatly enhances signal fidelity. The author has found this auxiliary impedance matching capability indispensible for correcting aberrations peculiar to commercial transducer assemblies. Impedance adjustments at both ends of the cable provide a means to compensate for the effects of electronic and acoustic reverberations.

It is worth becomming familiar with the renegade waveforms shown in the examples given herein. Any waveform having pronounced asymmetry or excess ringdown oscillations should be suspect unless it is recovered from a material sample known to introduce distortions (as with coarse grains, laminations, etc.). Illustrative examples of acceptable and unacceptable waveforms produced by varying the auxiliary damping resistance, and hence the degree of cable impedance matching, appear in figure 12. Any adjustment in coupling, bonding, and cable impedance matching will, of course, change the "system" modulation transfer characteristic. However, these adjustments are discretionary and should be made for convenience in subsequent deconvolutions of signals recovered from specimen materials.

CONCLUSIONS

Computer synthesis was used to simulate thin couplant and bond-layer effects associated with broadband ultrasonic transducers. It was shown that these thin layers in the acoustic path can produce distortions in ultrasonic signals and that these distortions become apparent and serious in the frequency regime from approximately 20 to 80 MHz. Selected examples are given to illustrate the potentially adverse effects of thin layers and practical approaches to recognizing and minimizing these effects. The results support the following conclusions:

1. When couplant or bond-layer acoustic impedances are significantly less than those of both of the contiguous materials joined (as with quartz, glycerine, and steel), the layer thickness should be less than 1 μm to avoid adverse signal distortion effects. This imposes a similar limitation on specimen surface flatness variations, which should be held to fractions of a micrometer in the transducer contact area.

2. The preceding tolerance limitation is removed when acoustic impedances of couplant or bond-layers are intermediate between those of the materials joined. In this case, exact matching of the layer and contiguous material acoustic impedance is unnecessary, and the layer thickness can exceed several tens of micrometers. In the cases illustrated, the signal is merely diminished by attenuation in the layer while distortions are minimized or absent.

3. Additional corrections to enhance signal fidelity can be made by inserting an auxiliary damping resistor in the transducer housing to complement an input damping resistor in the receiver housing and thereby compensate for adverse reverberation effects introduced by cable or transducer impedance mismatch effects.

The use of computer-simulated experimentation involving synthesized waveforms has clarified questions concerning multiple reverberation effects in thin layers. Additional work using this approach is recommended to study the effects of compound layers within transducers (relative to piezo-elements) and within material specimens (with lamellar microstructures).

ACKNOWLEDGEMENT

David R. Hull (Co-op student, University of Cincinnati) assisted in developing the waveform synthesis program used for this report.

REFERENCES

1. R. Truell, C. Elbaum, and B. B. Chick, Ultrasonic Methods in Solid State Physics, 1969, pp. 53-151 and 365-368. Academic Press, New York, NY.

2. E. P. Papadakis, "Ultrasonic Velocity and Attenuation: Measurement Methods with Scientific and Industrial Applications," Physical Acoustics - Principles and Methods, Vol. XII, Chapt. 5, 1976, p. 277. Academic Press, New York, NY.

3. A. Vary, "Ultrasonic Measurement of Material Properties," Research Techniques in Nondestructive Testing, Vol. IV, Chapt. 5, 1980, p. 160. Academic Press, London.

4. A. Vary, "Correlations Among Ultrasonic Propagation Factors and Fracture Toughness Properties of Metallic Materials," Materials Evaluation, Vol. 36, June 1978, pp. 55-64.

5. A. Vary, "Computer Signal Processing for Ultrasonic Attenuation and Velocity Measurements for Material Property Characterizations," NASA TM-79180 (1979).

6. J. H. Williams, Jr., H. Nayeb-Hashemi, and S. S. Lee, "Ultrasonic Attenuation and Velocity in AS/3501-6 Graphite/Epoxy Fiber Composite," NASA CR-3180 (1979).

7. K. F. Bainton and M. G. Silk, "Some Factors Which Affect the Performance of Ultrasonic Transducers," British Journal of Non-Destructive Testing, Vol. 22, Jan. 1980, pp. 15-20.

8. G. Bradfield, "Ultrasonic Transducers - 1. Ultrasonics, Vol. 8, July 1970, pp. 177-189.

9. J. Krautkramer and H. Krautkramer, Ultrasonic Testing of Materials, 1969, pp. 20-27 and 100-130. Springer-Verlag, New York, NY.

TABLE I. - SCHEDULE OF MATERIAL CONFIGURATIONS ANALYZED FOR THIN-LAYER ENERGY TRANSFER AND MULTIPLE-REFLECTION EFFECTS[a]

Principal variable[b]	Parametric relation[c]	Material sequenced[d]			Results, figure -
		[1]	[2]	[3]	
Couplant thickness	$Z_1 > Z_2 < Z_3$	Buffer (quartz)	Couplant (glycerine)	Specimen (steel)	4(a)-(l)
	$Z_1 < Z_2 < Z_3$	Buffer (quartz)	Couplant (fluid-X)	Specimen (steel)	5(a)-(f)
	$Z_1 < Z_2 < Z_3$	Buffer (acrylic)	Couplant (M-iodide)	Specimen (steel)	6(a)-(f)
Bond-layer thickness	$Z_1 > Z_2 < Z_3$	Piezoelement (PZT)	Bond (epoxy)	Buffer (quartz)	7(a)-(l)
	$Z_1 > Z_2 > Z_3$	Piezoelement (PZT)	Bond (W-epoxy)	Buffer (quartz)	8(a)-(f)
Bond-layer thickness	$Z_1 > Z_2 < Z_3$	Absorber (W-epoxy)	Bond (epoxy)	Piezoelement (PZT)	9(a)-(i)
	$Z_1 < Z_2 < Z_3$	Absorber (W-epoxy)	Bond (W-epoxy)	Piezoelement (PZT)	10(a)-(f)

[a]Results cover nominal range from 20 to 80 MHz centered at 50 MHz.
[b]Thin-layer thickness ranges from zero to 40 μm at 2-μm steps.
[c]Acoustic impedance, Z, is the product of density by (longitudinal) velocity.
[d]Material properties and further identification appear in table II.

TABLE II. - SELECTED MATERIALS, ACOUSTIC PROPERTIES, AND FUNCTIONS

Function	Material[a]	Density,[b] g/cm^3	Velocity[c] cm/μsec	Impedance[d] g/cm^{2}μsec
Piezoelectric transduction element	PZT (4 or 5) lead-zirconate niobate ceramic	7.5 (7.5-7.7)	0.395 (0.38-0.41)	3.0 (2.8-3.2)
Absorber, piezoelement backing	W-epoxy, 40 to 50 percent tungsten powder in epoxy resin	11 & 12 (10-13)	0.21 (0.17-0.24)	2.3 & 2.5 (1.7-3.1)
Adhesive bond	Epoxy resin	1.22 (1.1-1.3)	0.26 (0.24-0.28)	0.32 (0.28-0.36)
Buffer, delay	Fused quartz, quartz glass Acrylic resin	2.20 1.18	0.595 (0.59-0.60) (0.267-0.27)	1.31 (1.30-1.31) (0.315-0.319)
Couplant	Glycerine Methylene iodide Water (20° C)	1.26 3.33 1.00	0.192 .098 .148	0.242 .326 .148
Specimen	Mild steel Stainless steel Maraging steel	7.85 7.72 8.03	0.596 .598 .55	4.68 4.62 4.4

[a]Tabulation is limited to materials selected as representative for the purposes of this report in illustrating thin-layer effects.
[b]Property values not in parentheses are used for illustrative cases, parenthetical values are quoted to indicate actual range of variation.
[c]Longitudinal (compressional) ultrasonic wave velocity.
[d]Acoustic impedance, Z, equals product of density and velocity.

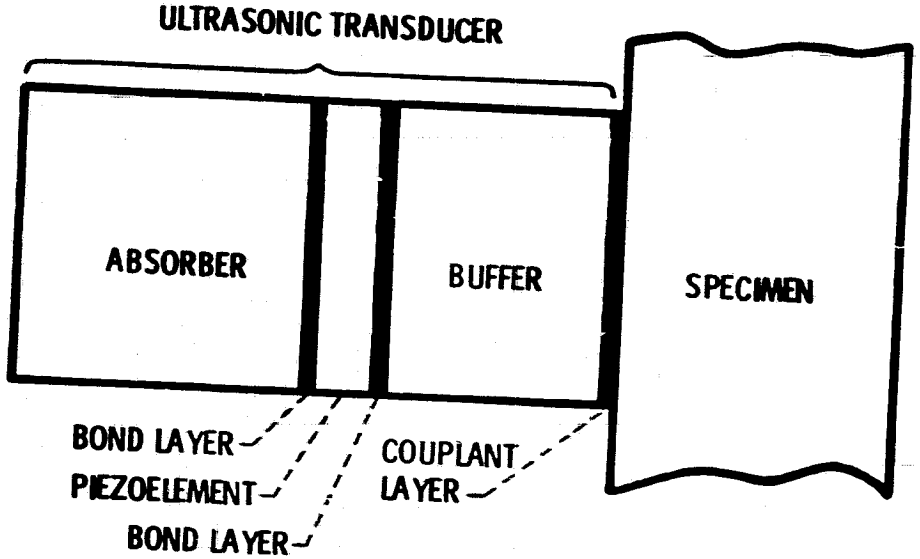

Figure 1. - Diagram of principal components involved in analysis of thin layer reverberations associated with broadband ultrasonic transducers.

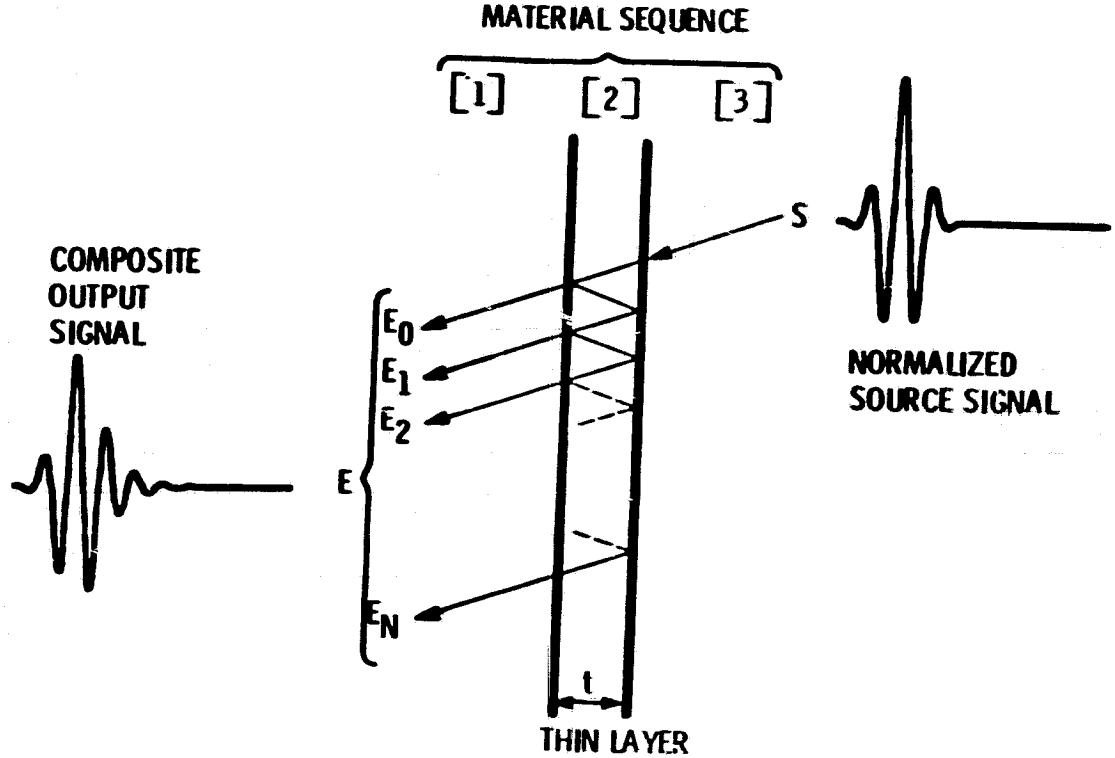

Figure 2. - Diagram of echo system. Ultrasonic signal S arrising in material [3] emerges in material [1] as a composite signal E resulting from superposition of multiple reflections in thin layer [2].

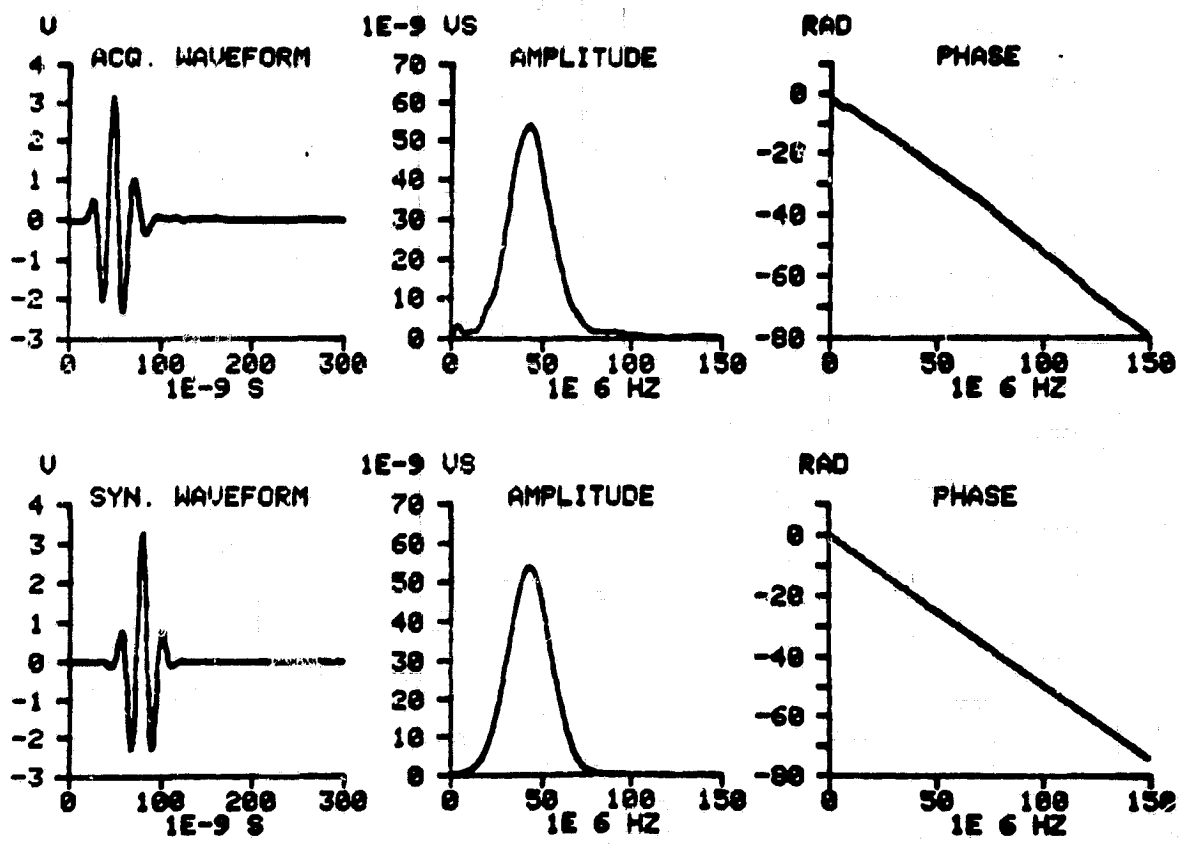

Figure 3. - Time and frequency domain versions of acquired ultrasonic waveform (top graphs) used as model for synthesized waveform (bottom graphs).

THIN LAYER ENERGY TRANSFER AND INTERFERENCE EFFECTS AT 50 MHZ

MATERIAL SYSTEM SEQUENCE	DENSITY (G/CM^3)	VELOCITY (CM/US)	IMPEDANCE (G/CM^{2}US)
[1] FUSED QUARTZ (BUFFER)	2.2	.595	1.309
[2] GLYCERINE (COUPLANT)	1.26	.192	.24192
[3] STEEL (SPECIMEN)	7.85	.596	4.6706

THIN LAYER [2] ATTENUATION COEFFICIENT = 60 NP/CM (AT 50 MHZ)

COMPOSITE SIGNAL RMS ENERGY (SOLID CURVES) & ATTENUATION (DOTTED CURVE)

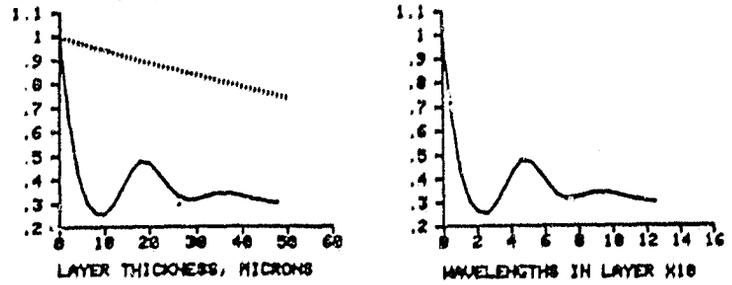

(a)

[1] FUSED QUARTZ (BUFFER) [2] GLYCERINE (COUPLANT) [3] STEEL (SPECIMEN)

LAYER [2] THICKNESS = 0 MICRON
WAVELENGTHS IN LAYER = 0
AT NOMINAL FREQUENCY = 50 MHZ
LAYER DELAY = 0 NANOSEC
OUT/IN AMPLITUDE = .437237
RMS ENERGY LEVEL = 1
PEAK FREQUENCY = 50 MHZ
SPECTRAL SKEWING = 0 %

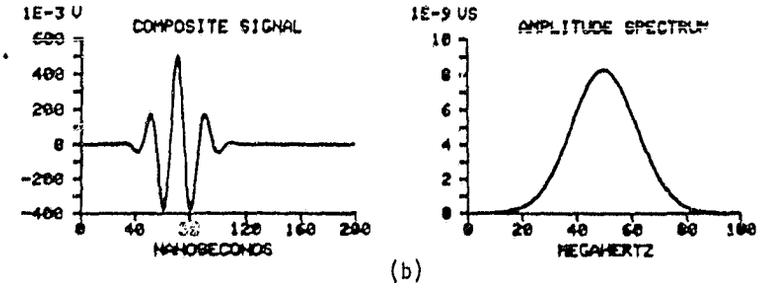

(b)

LAYER [2] THICKNESS = 2 MICRON
WAVELENGTHS IN LAYER = .0520833
AT NOMINAL FREQUENCY = 50 MHZ
LAYER DELAY = 2.08333 NANOSEC
OUT/IN AMPLITUDE = .272153
RMS ENERGY LEVEL = .610224
PEAK FREQUENCY = 48 MHZ
SPECTRAL SKEWING = -4 %

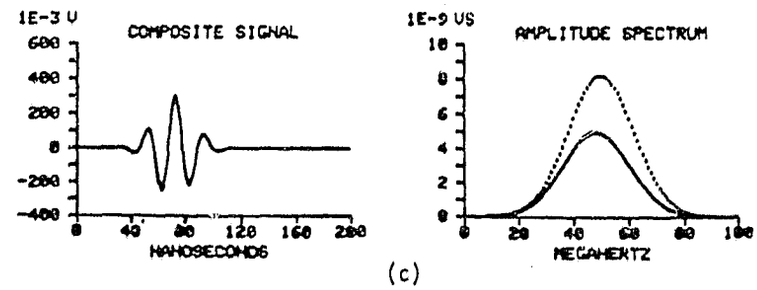

(c)

Figure 4. - Degeneration of composite signal and its frequency spectrum as glycerine couplant layer thickness between quartz buffer and steel specimen increases from 0 to 38 micron. Illustration of case where layer impedance is less than that of either contiguous material.

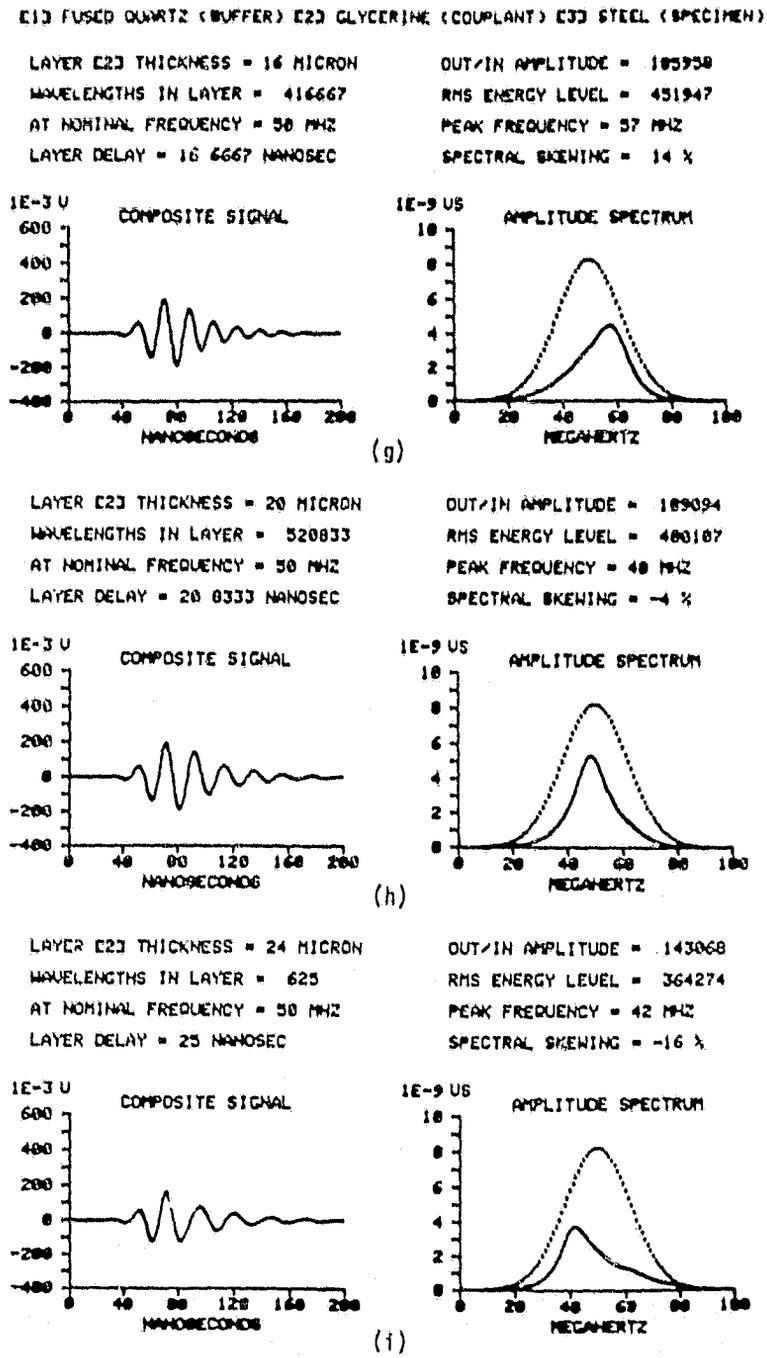

Figure 4. - Continued.

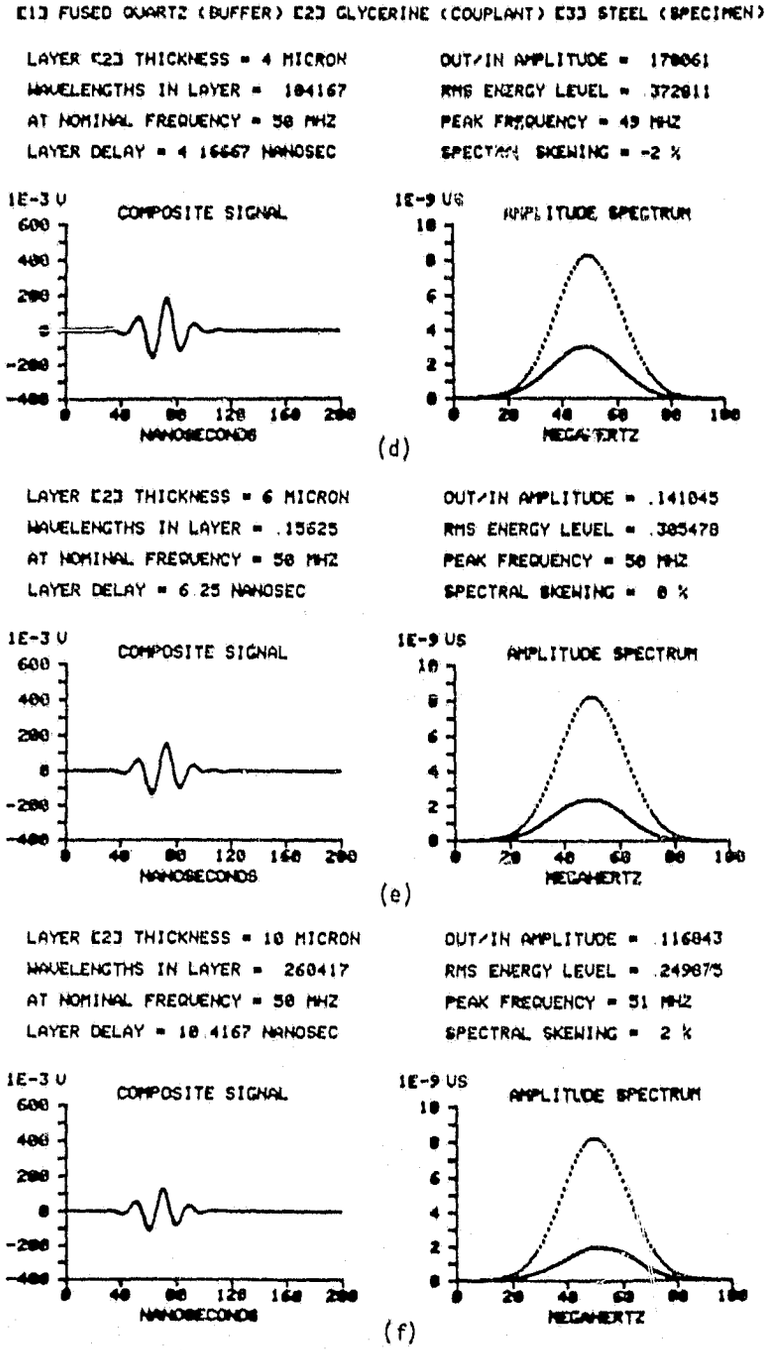

Figure 4. - Continued.

[1] FUSED QUARTZ (BUFFER) [2] GLYCERINE (COUPLANT) [3] STEEL (SPECIMEN)

LAYER [2] THICKNESS = 30 MICRON
WAVELENGTHS IN LAYER = 78125
AT NOMINAL FREQUENCY = 50 MHZ
LAYER DELAY = 31 25 NANOSEC

OUT/IN AMPLITUDE = 136343
RMS ENERGY LEVEL = .31467
PEAK FREQUENCY = 62 MHZ
SPECTRAL SKEWING = 24 %

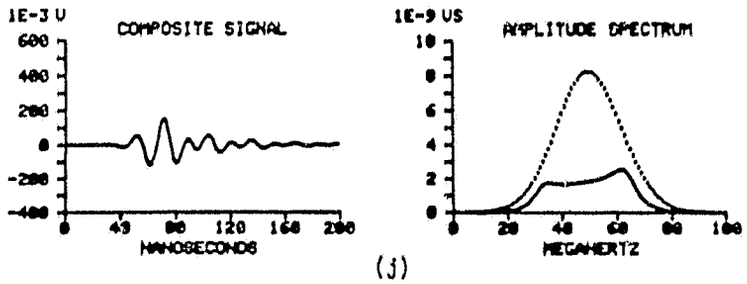

(j)

LAYER [2] THICKNESS = 34 MICRON
WAVELENGTHS IN LAYER = 685416
AT NOMINAL FREQUENCY = 50 MHZ
LAYER DELAY = 35 4167 NANOSEC

OUT/IN AMPLITUDE = .136162
RMS ENERGY LEVEL = .341745
PEAK FREQUENCY = 56 MHZ
SPECTRAL SKEWING = 12 %

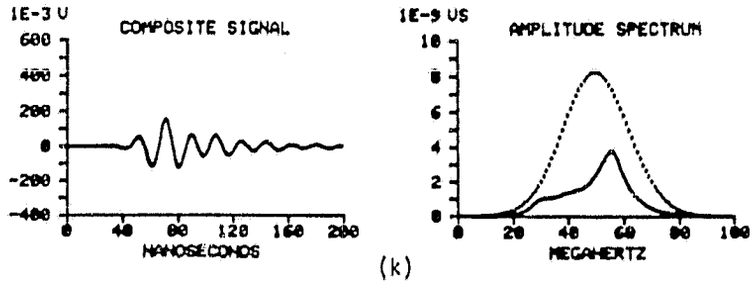

(k)

LAYER [2] THICKNESS = 38 MICRON
WAVELENGTHS IN LAYER = 989583
AT NOMINAL FREQUENCY = 50 MHZ
LAYER DELAY = 39 5833 NANOSEC

OUT/IN AMPLITUDE = .134407
RMS ENERGY LEVEL = .341605
PEAK FREQUENCY = 50 MHZ
SPECTRAL SKEWING = 0 %

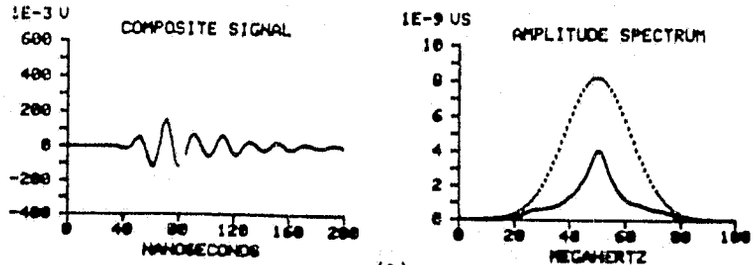

(l)

Figure 4. - Concluded.

THIN LAYER ENERGY TRANSFER AND INTERFERENCE EFFECTS AT 50 MHZ

MATERIAL SYSTEM SEQUENCE	DENSITY (G/CM^3)	VELOCITY (CM/US)	IMPEDANCE (G/CM^2US)
[1] FUSED QUARTZ (BUFFER)	2 2	5 5	1 389
[2] FLUID-X (COUPLANT)	3	3	1 5
[3] STEEL (SPECIMEN)	7 85	5 96	4 6786

THIN LAYER [2] ATTENUATION COEFFICIENT = 50 NP/CM (AT 50 MHZ)

COMPOSITE SIGNAL RMS ENERGY (SOLID CURVES) & ATTENUATION (DOTTED CURVE)

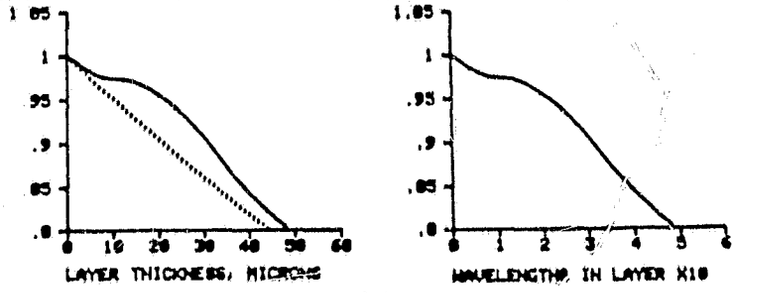

(a)

[1] FUSED QUARTZ (BUFFER) [2] FLUID-X (COUPLANT) [3] STEEL (SPECIMEN)

LAYER [2] THICKNESS = 0 MICRON
WAVELENGTHS IN LAYER = 0
AT NOMINAL FREQUENCY = 50 MHZ
LAYER DELAY = 0 NANOSEC

OUT/IN AMPLITUDE = .437237
RMS ENERGY LEVEL = 1
PEAK FREQUENCY = 50 MHZ
SPECTRAL SKEWING = 0 %

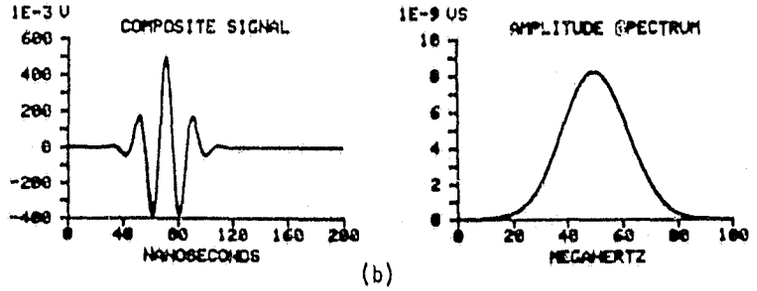

(b)

LAYER [2] THICKNESS = 2 MICRON
WAVELENGTHS IN LAYER = 02
AT NOMINAL FREQUENCY = 50 MHZ
LAYER DELAY = .8 NANOSEC

OUT/IN AMPLITUDE = .433913
RMS ENERGY LEVEL = .992232
PEAK FREQUENCY = 50 MHZ
SPECTRAL SKEWING = 0 %

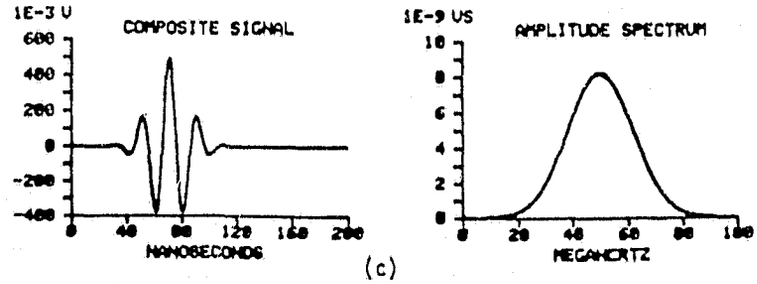

(c)

Figure 5. - Variation of composite signal and its frequency spectrum as couplant layer thickness between quartz buffer and steel specimen increases from 0 to 30 micron. Illustration of case where layer impedance is intermediate between that of contiguous materials.

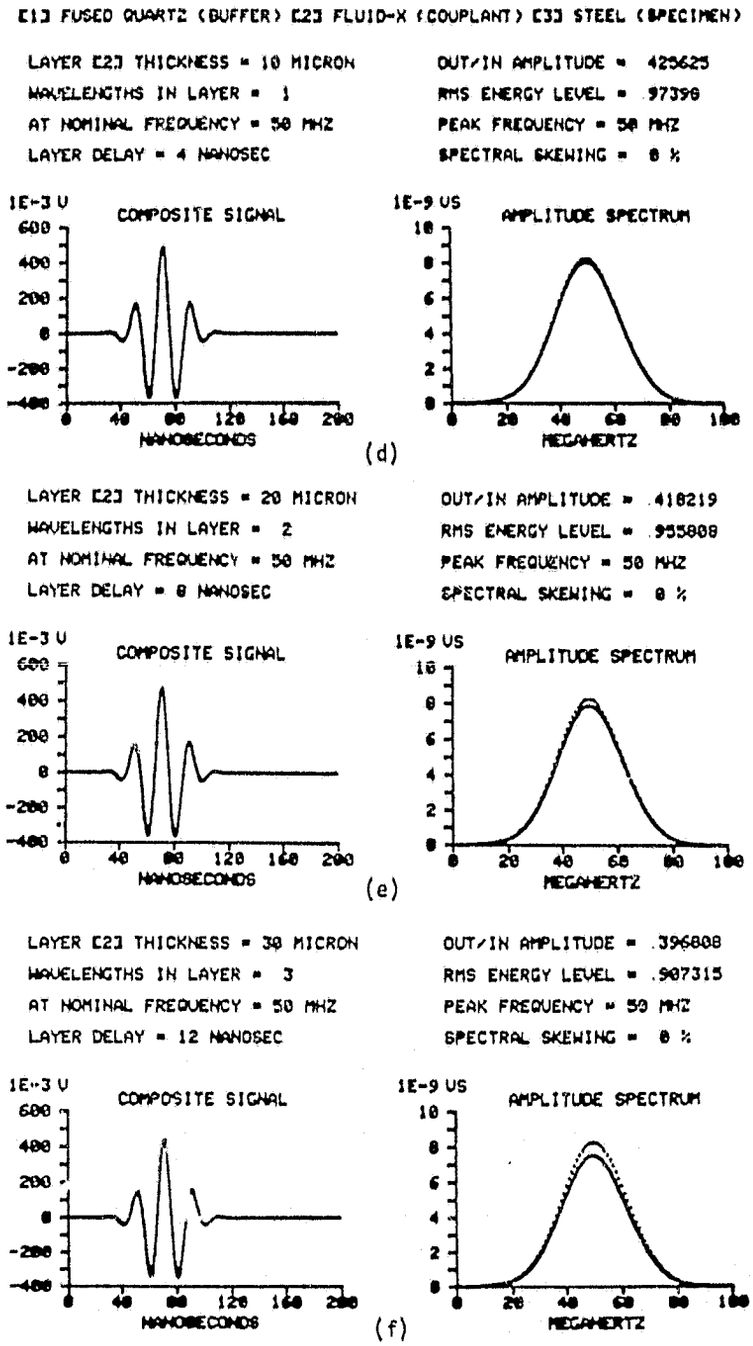

Figure 5. - Concluded.

THIN LAYER ENERGY TRANSFER AND INTERFERENCE EFFECTS AT 50 MHZ

MATERIAL SYSTEM SEQUENCE	DENSITY (G/CM^3)	VELOCITY (CM/US)	IMPEDANCE (G/CM^2US)
[1] ACRYLIC (BUFFER)	1.10	.27	.3186
[2] M-IODIDE (COUPLANT)	3.33	.098	.32634
[3] STEEL (SPECIMEN)	7.85	.596	4.6786

THIN LAYER [2] ATTENUATION COEFFICIENT = 60 NP/CM (AT 50 MHZ)

COMPOSITE SIGNAL RMS ENERGY (SOLID CURVES) & ATTENUATION (DOTTED CURVE)

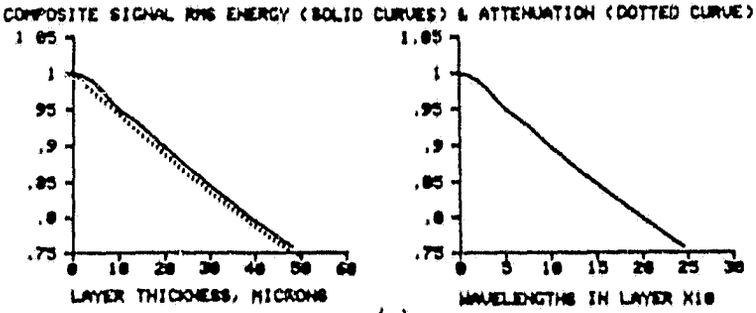

(a)

[1] ACRYLIC (BUFFER) [2] METHYLENE IODIDE (COUPLANT) [3] STEEL (SPECIMEN)

LAYER [2] THICKNESS = 0 MICRON
WAVELENGTHS IN LAYER = 0
AT NOMINAL FREQUENCY = 50 MHZ
LAYER DELAY = 0 NANOSEC

OUT/IN AMPLITUDE = .127511
RMS ENERGY LEVEL = 1
PEAK FREQUENCY = 50 MHZ
SPECTRAL SKEWING = 0 %

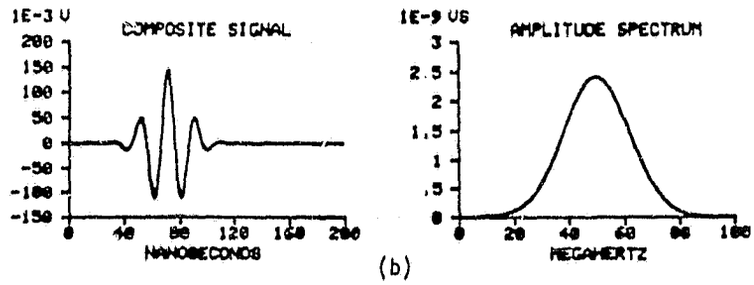

(b)

LAYER [2] THICKNESS = 2 MICRON
WAVELENGTHS IN LAYER = .182041
AT NOMINAL FREQUENCY = 50 MHZ
LAYER DELAY = 4.00163 NANOSEC

OUT/IN AMPLITUDE = .126859
RMS ENERGY LEVEL = .995003
PEAK FREQUENCY = 50 MHZ
SPECTRAL SKEWING = 0 %

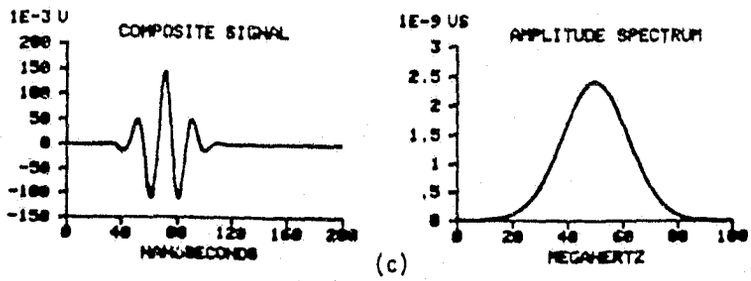

(c)

Figure 6. - Variation of composite signal and its frequency spectrum as couplant layer thickness between acrylic buffer and steel specimen increases from 0 to 30 micron. Illustration of case where layer impedance is intermediate between that of contiguous materials.

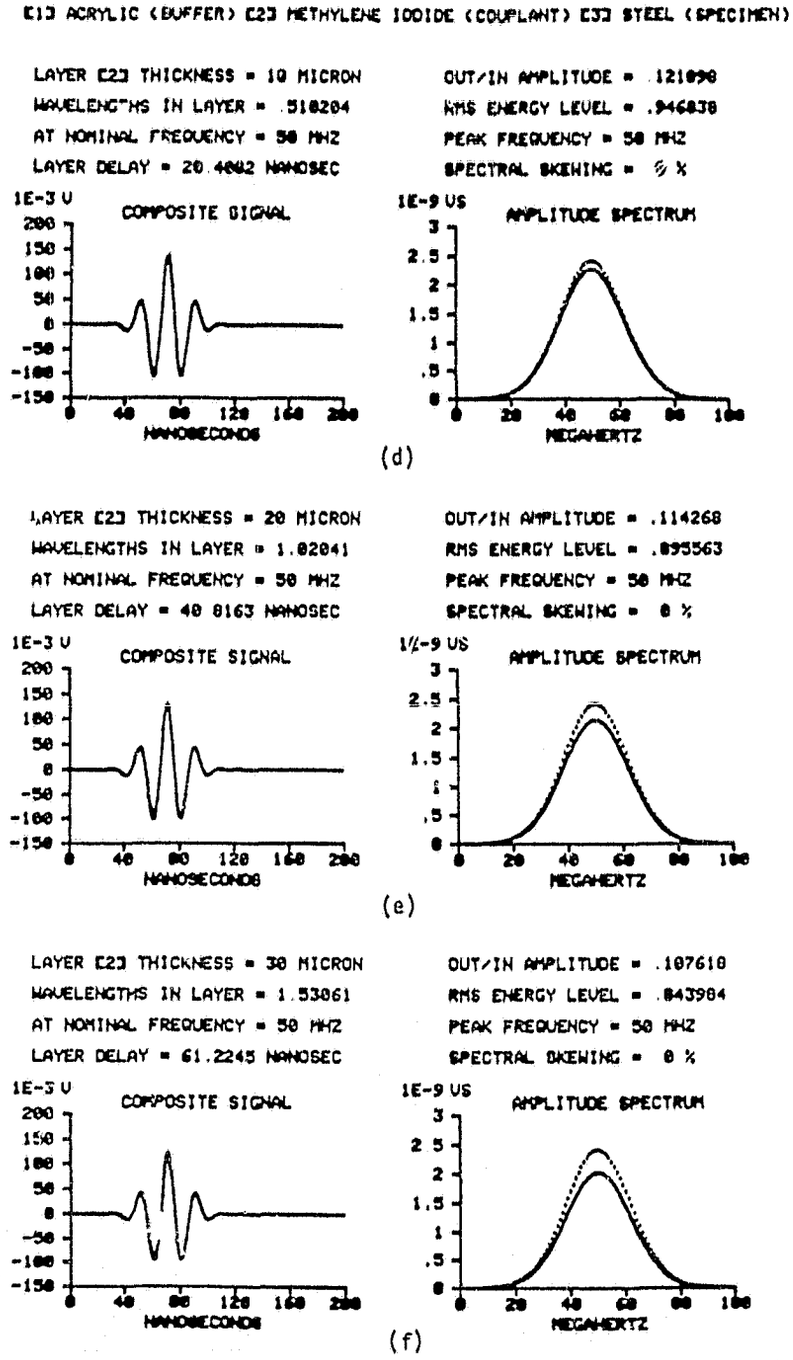

Figure 6. - Concluded.

THIN LAYER ENERGY TRANSFER AND INTERFERENCE EFFECTS AT 50 MHZ

MATERIAL SYSTEM SEQUENCE	DENSITY (G/CM^3)	VELOCITY (CM/US)	IMPEDANCE (G/CM^2US)
[1] PZT (PIEZOELEMENT)	7.6	395	3.002
[2] EPOXY (BOND)	1.22	.26	.3172
[3] FUSED QUARTZ (BUFFER)	2.2	.595	1.309

THIN LAYER [2] ATTENUATION COEFFICIENT = 20 NP/CM (AT 50 MHZ)

COMPOSITE SIGNAL RMS ENERGY (SOLID CURVES) & ATTENUATION (DOTTED CURVE):

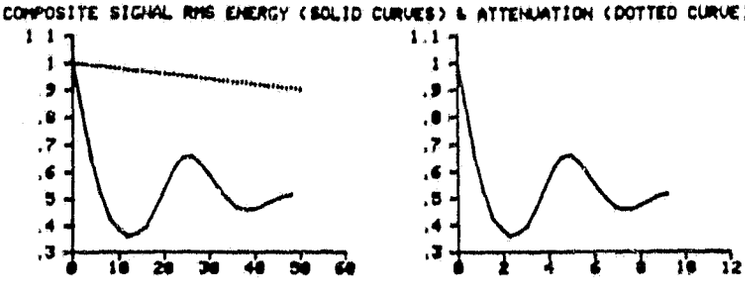

(a)

[1] PZT (PIEZOELEMENT) [2] EPOXY (BOND) [3] FUSED QUARTZ (BUFFER)

LAYER [3] THICKNESS = 0 MICRON
WAVELENGTHS IN LAYER = 0
AT NOMINAL FREQUENCY = 50 MHZ
LAYER DELAY = 0 NANOSEC

OUT/IN AMPLITUDE = 1.39272
RMS ENERGY LEVEL = 1
PEAK FREQUENCY = 50 MHZ
SPECTRAL SKEWING = 0 %

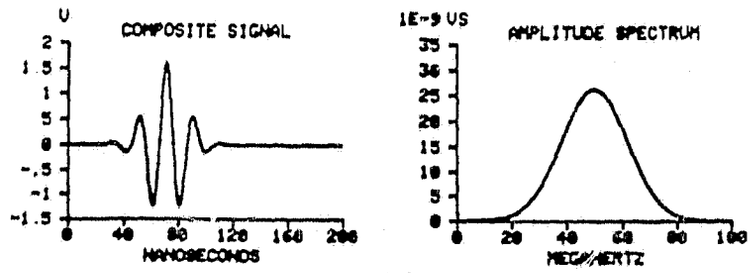

(b)

LAYER [2] THICKNESS = 2 MICRON
WAVELENGTHS IN LAYER = .0384615
AT NOMINAL FREQUENCY = 50 MHZ
LAYER DELAY = 1.53846 NANOSEC

OUT/IN AMPLITUDE = 1.15028
RMS ENERGY LEVEL = .826200
PEAK FREQUENCY = 49 MHZ
SPECTRAL SKEWING = -2 %

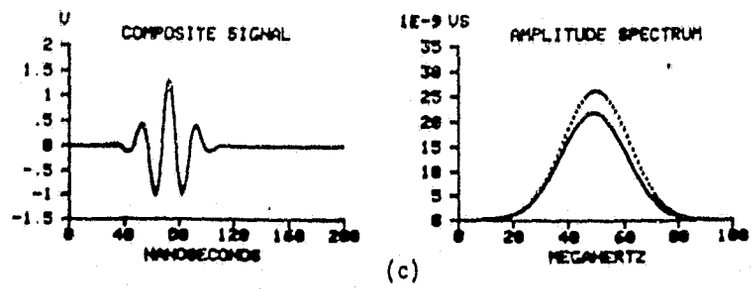

(c)

Figure 7. - Degeneration of composite signal and its frequency spectrum as bond layer thickness between PZT piezoelement and quartz buffer increases from 0 to 38 micron. Illustration of case where layer impedance is less than that of either contiguous material.

[1] PZT (PIEZOELEMENT) [2] EPOXY (BOND) [3] FUSED QUARTZ (BUFFER)

LAYER [2] THICKNESS = 4 MICRON
WAVELENGTHS IN LAYER = .0769231
AT NOMINAL FREQUENCY = 50 MHZ
LAYER DELAY = 3.07692 NANOSEC

OUT/IN AMPLITUDE = .694238
RMS ENERGY LEVEL = .635153
PEAK FREQUENCY = 49 MHZ
SPECTRAL SKEWING = -2 %

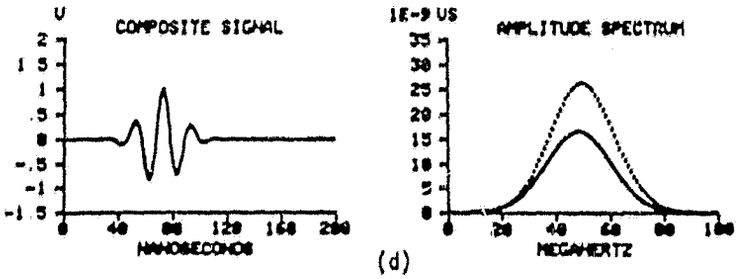

(d)

LAYER [2] THICKNESS = 6 MICRON
WAVELENGTHS IN LAYER = .115385
AT NOMINAL FREQUENCY = 50 MHZ
LAYER DELAY = 4.61538 NANOSEC

OUT/IN AMPLITUDE = .677442
RMS ENERGY LEVEL = .476912
PEAK FREQUENCY = 48 MHZ
SPECTRAL SKEWING = -4 %

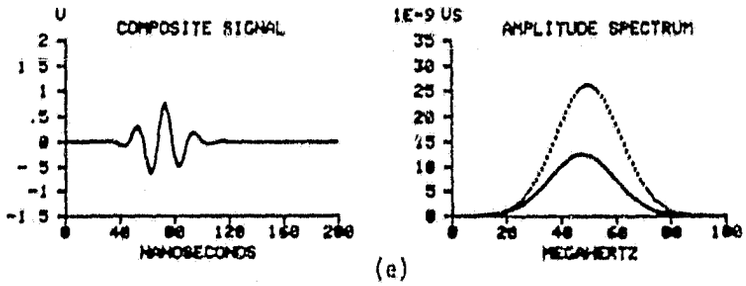

(e)

LAYER [2] THICKNESS = 10 MICRON
WAVELENGTHS IN LAYER = .192308
AT NOMINAL FREQUENCY = 50 MHZ
LAYER DELAY = 7.69231 NANOSEC

OUT/IN AMPLITUDE = .53392
RMS ENERGY LEVEL = .364316
PEAK FREQUENCY = 49 MHZ
SPECTRAL SKEWING = -2 %

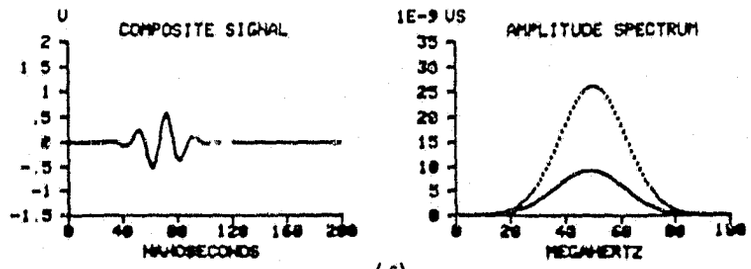

(f)

Figure 7. - Continued.

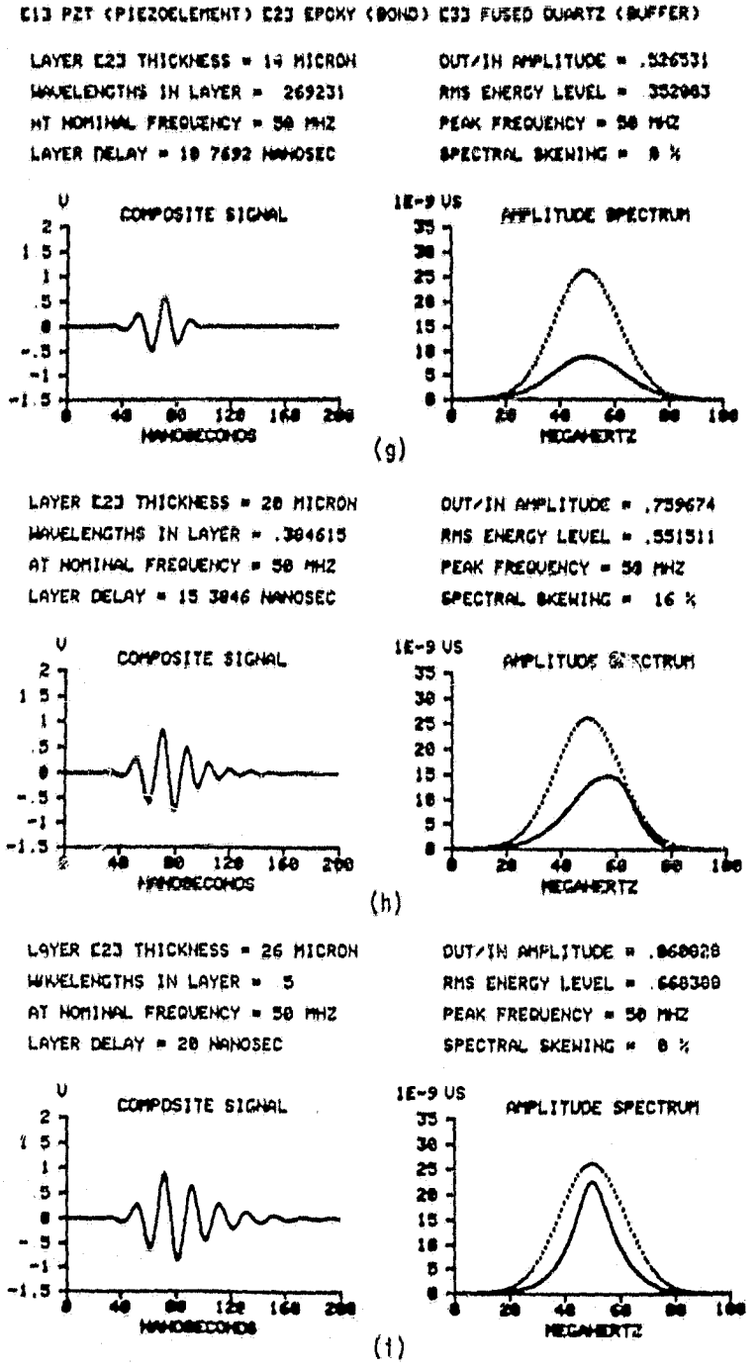

Figure 7. - Continued.

[3] PZT (PIEZOELEMENT) [2] EPOXY (BOND) [3] FUSED QUARTZ (BUFFER)

LAYER [2] THICKNESS = 30 MICRON
WAVELENGTHS IN LAYER = .576923
AT NOMINAL FREQUENCY = 50 MHZ
LAYER DELAY = 23.6769 NANOSEC

OUT/IN AMPLITUDE = .72732
RMS ENERGY LEVEL = .501745
PEAK FREQUENCY = 45 MHZ
SPECTRAL SKEWING = -18 %

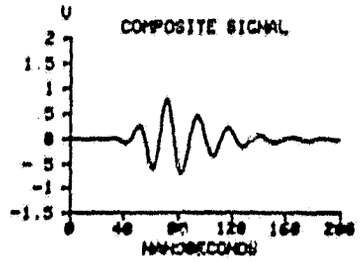

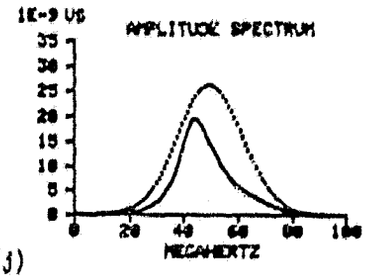

(j)

LAYER [2] THICKNESS = 34 MICRON
WAVELENGTHS IN LAYER = .653846
AT NOMINAL FREQUENCY = 50 MHZ
LAYER DELAY = 26.1538 NANOSEC

OUT/IN AMPLITUDE = .648973
RMS ENERGY LEVEL = .48737
PEAK FREQUENCY = 40 MHZ
SPECTRAL SKEWING = -20 %

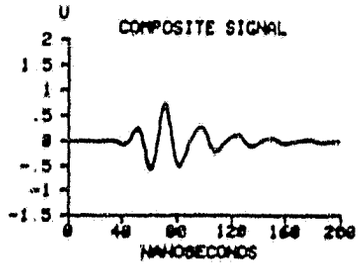

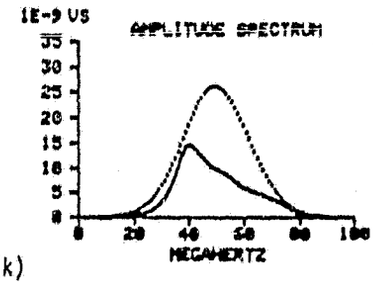

(k)

LAYER [2] THICKNESS = 38 MICRON
WAVELENGTHS IN LAYER = .730769
AT NOMINAL FREQUENCY = 50 MHZ
LAYER DELAY = 29.2308 NANOSEC

OUT/IN AMPLITUDE = .638462
RMS ENERGY LEVEL = .451203
PEAK FREQUENCY = 37 MHZ
SPECTRAL SKEWING = -26 %

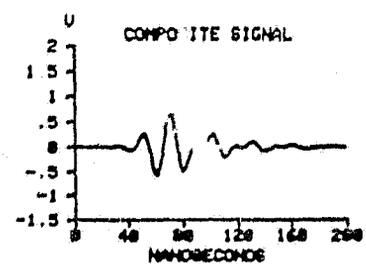

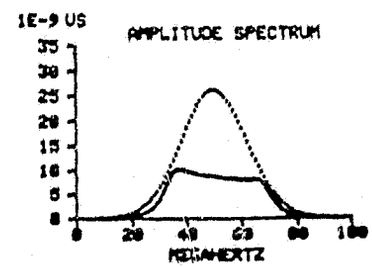

(l)

Figure 7. - Concluded.

THIN LAYER ENERGY TRANSFER AND INTERFERENCE EFFECTS AT 50 MHZ

MATERIAL SYSTEM SEQUENCE	DENSITY (G/CM^3)	VELOCITY (CM/US)	IMPEDANCE (G/CM^2US)
[1] PZT (PIEZOELEMENT)	7.6	.395	3.002
[2] W-EPOXY (BOND)	1.2	.21	2.52
[3] FUSED QUARTZ (BUFFER)	2.2	.593	1.349

THIN LAYER [2] ATTENUATION COEFFICIENT = 25 NP/CM (AT 50 MHZ)

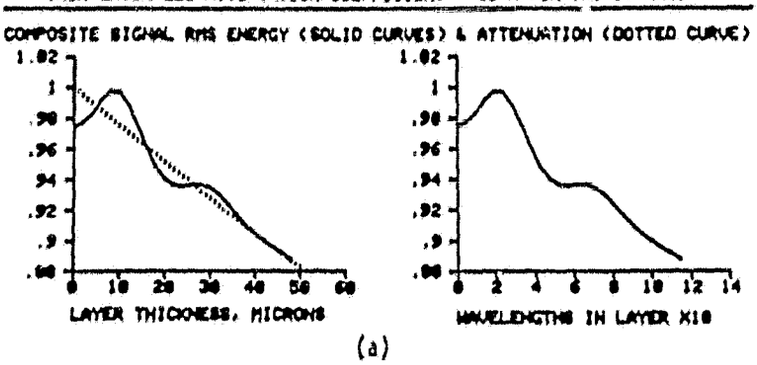

(a)

[1] PZT (PIEZOELEMENT) [2] W-EPOXY (BOND) [3] FUSED QUARTZ (BUFFER)

LAYER [2] THICKNESS = 0 MICRON
WAVELENGTHS IN LAYER = 0
AT NOMINAL FREQUENCY = 50 MHZ
LAYER DELAY = 0 NANOSEC

OUT/IN AMPLITUDE = 1.39272
RMS ENERGY LEVEL = 1
PEAK FREQUENCY = 50 MHZ
SPECTRAL SKEWING = 0 %

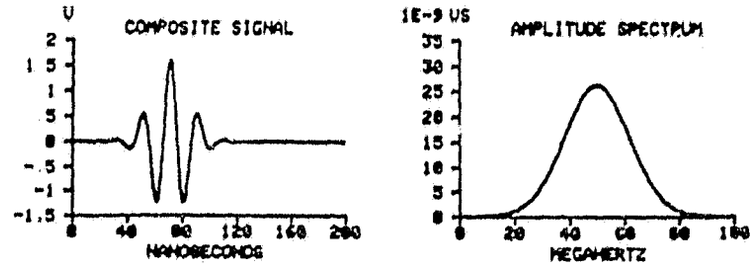

(b)

LAYER [2] THICKNESS = 2 MICRON
WAVELENGTHS IN LAYER = .047619
AT NOMINAL FREQUENCY = 50 MHZ
LAYER DELAY = 1.90476 NANOSEC

OUT/IN AMPLITUDE = 1.39315
RMS ENERGY LEVEL = 1.00013
PEAK FREQUENCY = 50 MHZ
SPECTRAL SKEWING = 0 %

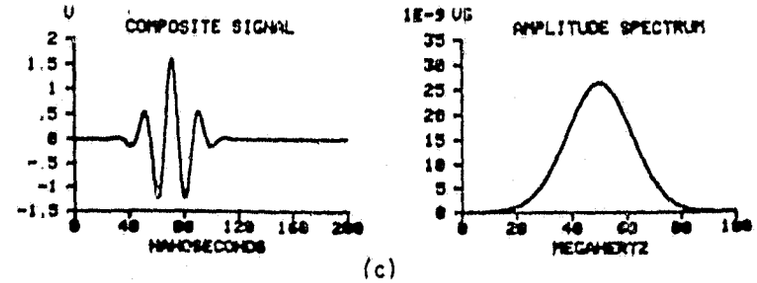

(c)

Figure 8. - Variation of composite signal and its frequency spectrum as bond layer thickness between PZT piezoelement and quartz buffer increases from 0 to 30 micron. Illustration of case where layer impedance is intermediate between that of contiguous materials.

[1] PZT (PIEZOELEMENT) [2] W-EPOXY (BOND) [3] FUSED QUARTZ (BUFFER)

LAYER [2] THICKNESS = 10 MICRON
WAVELENGTHS IN LAYER = .238095
AT NOMINAL FREQUENCY = 50 MHZ
LAYER DELAY = 9.52381 NANOSEC

OUT/IN AMPLITUDE = 1.43819
RMS ENERGY LEVEL = 1.02565
PEAK FREQUENCY = 50 MHZ
SPECTRAL SKEWING = 0 %

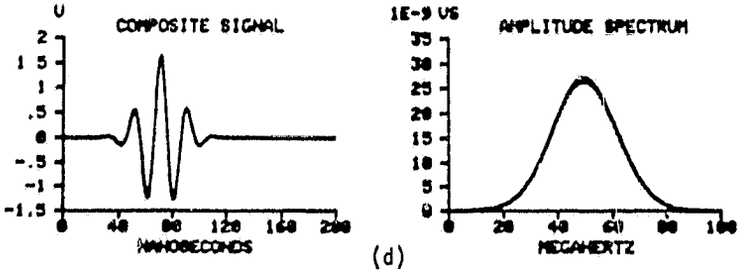

(d)

LAYER [2] THICKNESS = 20 MICRON
WAVELENGTHS IN LAYER = .47619
AT NOMINAL FREQUENCY = 50 MHZ
LAYER DELAY = 19.0476 NANOSEC

OUT/IN AMPLITUDE = 1.35321
RMS ENERGY LEVEL = .963689
PEAK FREQUENCY = 50 MHZ
SPECTRAL SKEWING = 0 %

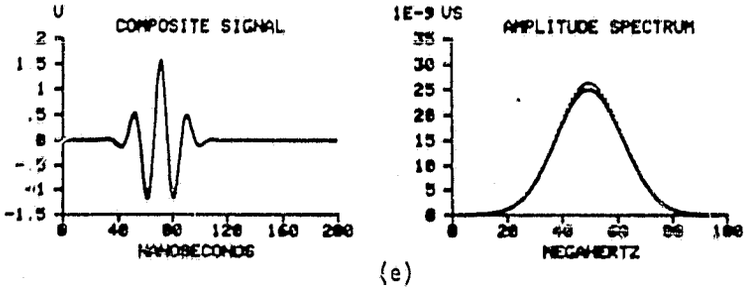

(e)

LAYER [2] THICKNESS = 30 MICRON
WAVELENGTHS IN LAYER = .714286
AT NOMINAL FREQUENCY = 50 MHZ
LAYER DELAY = 28.5714 NANOSEC

OUT/IN AMPLITUDE = 1.33262
RMS ENERGY LEVEL = .959687
PEAK FREQUENCY = 50 MHZ
SPECTRAL SKEWING = 0 %

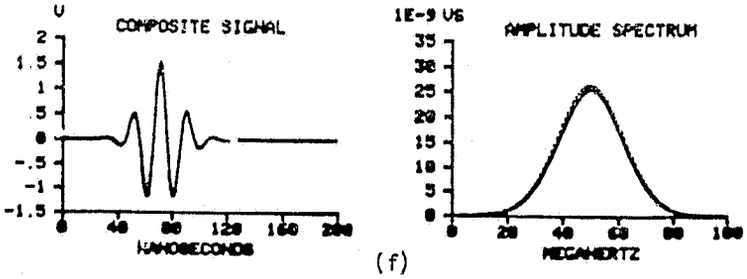

(f)

Figure 8. - Concluded.

THIN LAYER ENERGY TRANSFER AND INTERFERENCE EFFECTS AT 50 MHZ

MATERIAL SYSTEM SEQUENCE	DENSITY (G/CM^3)	VELOCITY (CM/US)	IMPEDANCE (G/CM^{2}US)
[1] W-EPOXY (ABSORBER)	11	.21	2.31
[2] EPOXY (BOND)	1.22	.26	.3172
[3] PZT (PIEZOELEMENT)	7.6	.395	3.002

THIN LAYER [2] ATTENUATION COEFFICIENT = 20 NP/CM (AT 50 MHZ)

COMPOSITE SIGNAL RMS ENERGY (SOLID CURVES) & ATTENUATION (DOTTED CURVE)

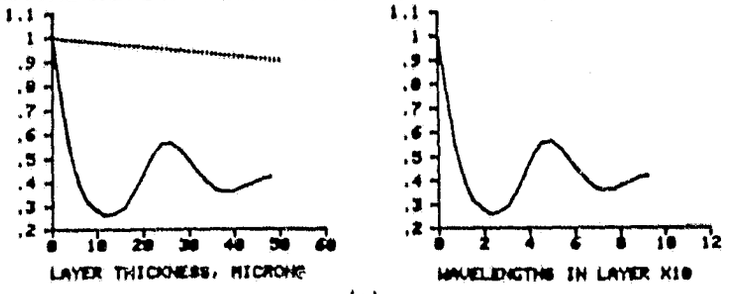

(a)

[1] W-EPOXY (ABSORBER) [2] EPOXY (BOND) [3] PZT (PIEZOELEMENT)

LAYER [2] THICKNESS = 0 MICRON
WAVELENGTHS IN LAYER = 0
AT NOMINAL FREQUENCY = 50 MHZ
LAYER DELAY = 0 NANOSEC

OUT/IN AMPLITUDE = .869729
RMS ENERGY LEVEL = 1
PEAK FREQUENCY = 50 MHZ
SPECTRAL SKEWING = 0 %

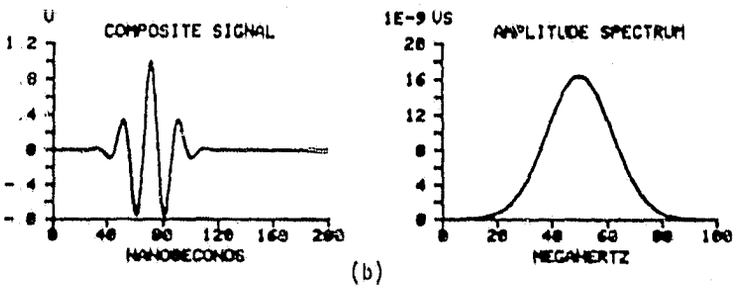

(b)

LAYER [2] THICKNESS = 2 MICRON
WAVELENGTHS IN LAYER = .0304615
AT NOMINAL FREQUENCY = 50 MHZ
LAYER DELAY = 1.53846 NANOSEC

OUT/IN AMPLITUDE = .642242
RMS ENERGY LEVEL = .737171
PEAK FREQUENCY = 49 MHZ
SPECTRAL SKEWING = -2 %

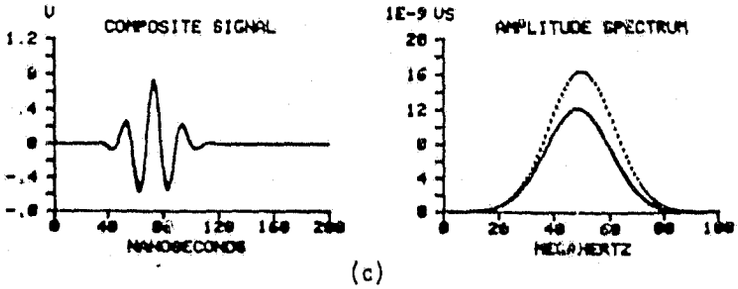

(c)

Figure 9. - Degeneration of composite signal and its frequency spectrum as bond layer thickness between tungsten-epoxy absorber and PZT piezoelement increases from 0 to 26 micron. Illustration of case where layer impedance is less than that of either contiguous material.

[1] W-EPOXY (ABSORBER) [2] EPOXY (BOND) [3] PZT (PIEZOELEMENT)

LAYER [2] THICKNESS = 4 MICRON
WAVELENGTHS IN LAYER = .0769231
AT NOMINAL FREQUENCY = 50 MHZ
LAYER DELAY = 3.07692 NANOSEC

OUT/IN AMPLITUDE = .446361
RMS ENERGY LEVEL = .494743
PEAK FREQUENCY = 49 MHZ
SPECTRAL SKEWING = -2 %

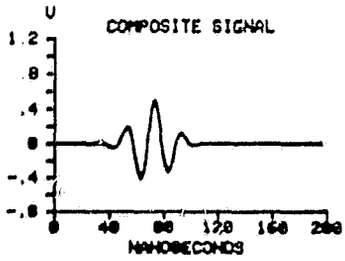

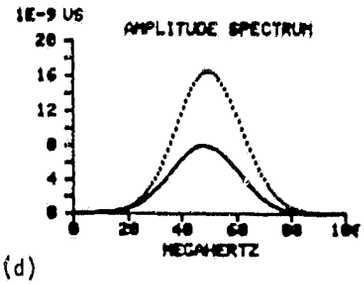

(d)

LAYER [2] THICKNESS = 6 MICRON
WAVELENGTHS IN LAYER = .115385
AT NOMINAL FREQUENCY = 50 MHZ
LAYER DELAY = 4.61538 NANOSEC

OUT/IN AMPLITUDE = .315181
RMS ENERGY LEVEL = .356727
PEAK FREQUENCY = 47 MHZ
SPECTRAL SKEWING = -6 %

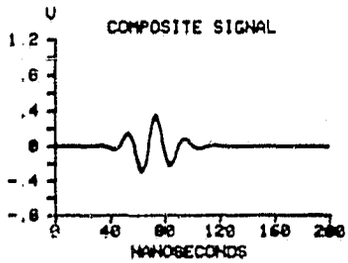

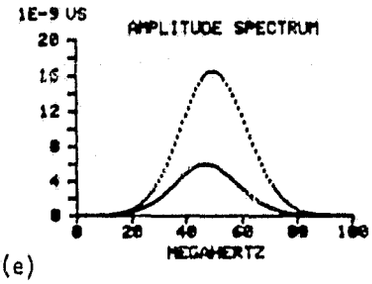

(e)

LAYER [2] THICKNESS = 10 MICRON
WAVELENGTHS IN LAYER = .192308
AT NOMINAL FREQUENCY = 50 MHZ
LAYER DELAY = 7.69231 NANOSEC

OUT/IN AMPLITUDE = .239925
RMS ENERGY LEVEL = .259472
PEAK FREQUENCY = 48 MHZ
SPECTRAL SKEWING = -4 %

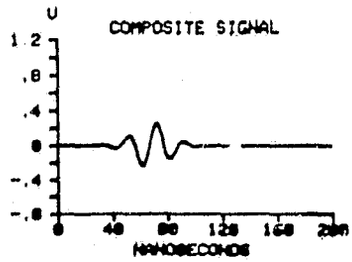

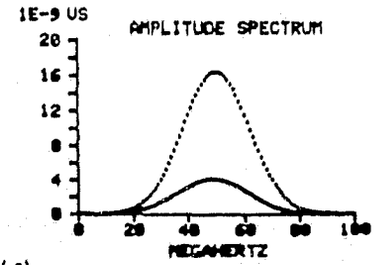

(f)

Figure 9. - Continued.

[1] W-EPOXY (ABSORBER) [2] EPOXY (BOND) [3] PZT (PIEZOELEMENT)

LAYER [2] THICKNESS = 14 MICRON
WAVELENGTHS IN LAYER = 269231
AT NOMINAL FREQUENCY = 50 MHZ
LAYER DELAY = 10.7692 NANOSEC

OUT/IN AMPLITUDE = .23642
RMS ENERGY LEVEL = .250415
PEAK FREQUENCY = 49 MHZ
SPECTRAL SKEWING = -2 %

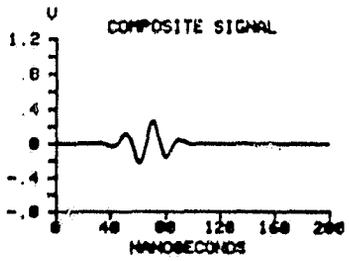

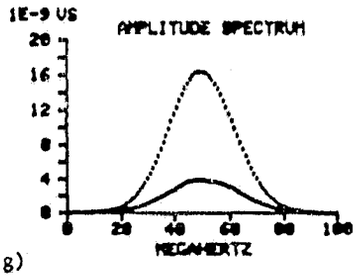

(g)

LAYER [2] THICKNESS = 20 MICRON
WAVELENGTHS IN LAYER = .384615
AT NOMINAL FREQUENCY = 50 MHZ
LAYER DELAY = 15.3846 NANOSEC

OUT/IN AMPLITUDE = .375897
RMS ENERGY LEVEL = .445712
PEAK FREQUENCY = 61 MHZ
SPECTRAL SKEWING = 22 %

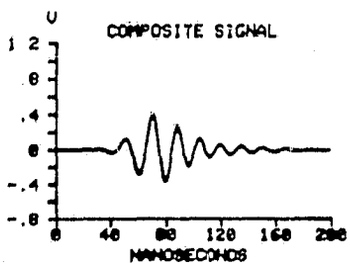

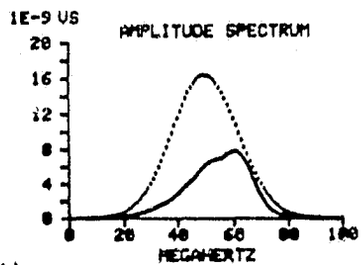

(h)

LAYER [2] THICKNESS = 26 MICRON
WAVELENGTHS IN LAYER = .5
AT NOMINAL FREQUENCY = 50 MHZ
LAYER DELAY = 20 NANOSEC

OUT/IN AMPLITUDE = .433281
RMS ENERGY LEVEL = .57284
PEAK FREQUENCY = 50 MHZ
SPECTRAL SKEWING = 0 %

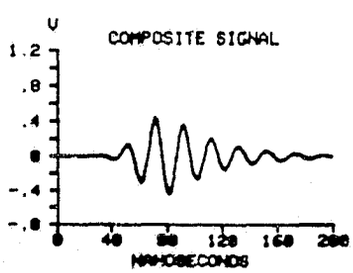

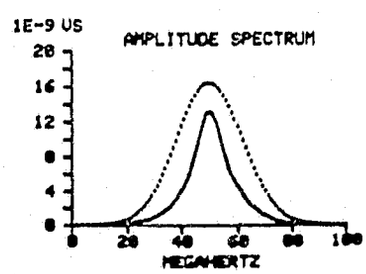

(i)

Figure 9. - Concluded.

THIN LAYER ENERGY TRANSFER AND INTERFERENCE EFFECTS AT 50 MHZ

MATERIAL SYSTEM SEQUENCE	DENSITY (G/CM^3)	VELOCITY (CM/US)	IMPEDANCE (G/CM^{2}US)
[1] W-EPOXY (ABSORBER)	11	.21	2.31
[2] W-EPOXY (BOND)	12	.21	2.52
[3] PZT (PIEZOELEMENT)	7.6	.395	3.002

THIN LAYER [2] ATTENUATION COEFFICIENT = 25 NP/CM (AT 50 MHZ)

COMPOSITE SIGNAL RMS ENERGY (SOLID CURVES) & ATTENUATION (DOTTED CURVE).

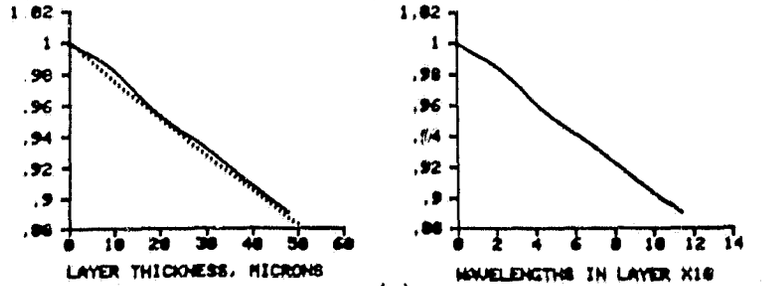

(a)

[1] W-EPOXY (ABSORBER) [2] W-EPOXY (BOND) [3] PZT (PIEZOELEMENT)

LAYER [2] THICKNESS = 0 MICRON
WAVELENGTHS IN LAYER = 0
AT NOMINAL FREQUENCY = 50 MHZ
LAYER DELAY = 0 NANOSEC

OUT/IN AMPLITUDE = .869729
RMS ENERGY LEVEL = 1
PEAK FREQUENCY = 50 MHZ
SPECTRAL SKEWING = 0 %

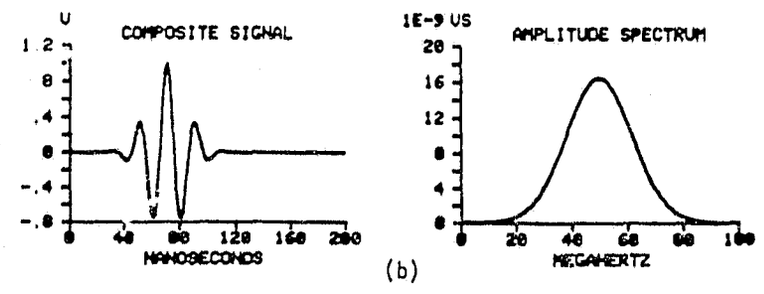

(b)

LAYER [2] THICKNESS = 2 MICRON
WAVELENGTHS IN LAYER = .047619
AT NOMINAL FREQUENCY = 50 MHZ
LAYER DELAY = 1.90476 NANOSEC

OUT/IN AMPLITUDE = .86686
RMS ENERGY LEVEL = .995744
PEAK FREQUENCY = 50 MHZ
SPECTRAL SKEWING = 0 %

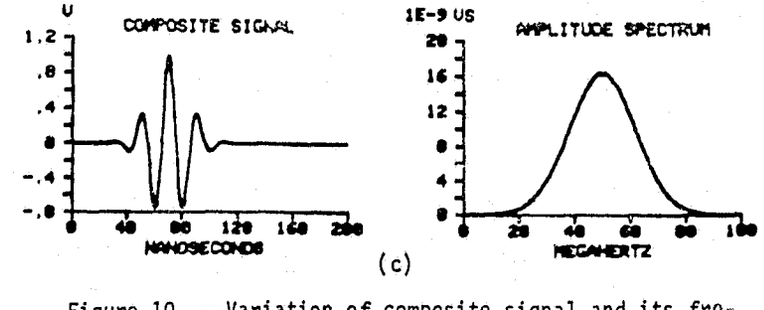

(c)

Figure 10. - Variation of composite signal and its frequency spectrum as bond layer thickness between tungsten-epoxy absorber and PZT piezoelement increases from 0 to 30 micron. Illustration of case where layer impedance is intermediate between that of contiguous materials.

[1] W-EPOXY (ABSORBER) [2] W-EPOXY (BOND) [3] PZT (PIEZOELEMENT)

LAYER [2] THICKNESS = 10 MICRON
WAVELENGTHS IN LAYER = 238095
AT NOMINAL FREQUENCY = 50 MHZ
LAYER DELAY = 9.52381 NANOSEC

OUT/IN AMPLITUDE = 853395
RMS ENERGY LEVEL = 982099
PEAK FREQUENCY = 50 MHZ
SPECTRAL SKEWING = 0 %

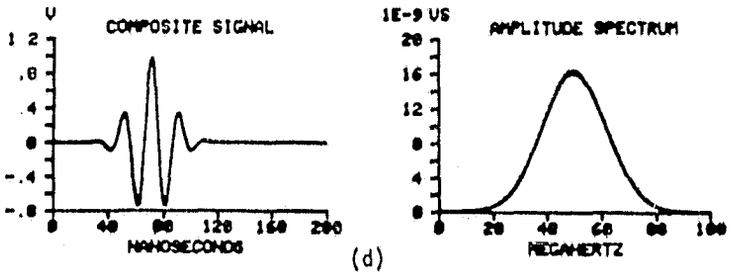

(d)

LAYER [2] THICKNESS = 20 MICRON
WAVELENGTHS IN LAYER = .47619
AT NOMINAL FREQUENCY = 50 MHZ
LAYER DELAY = 19.0476 NANOSEC

OUT/IN AMPLITUDE = .829767
RMS ENERGY LEVEL = .952956
PEAK FREQUENCY = 50 MHZ
SPECTRAL SKEWING = 0 %

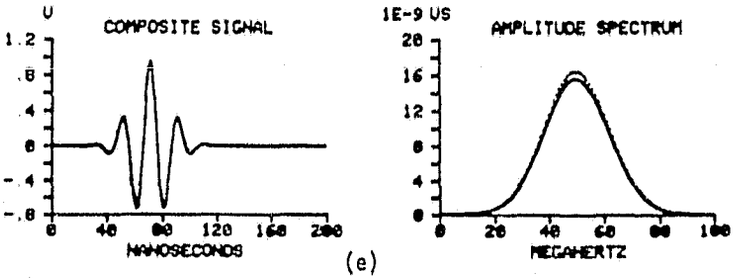

(e)

LAYER [2] THICKNESS = 30 MICRON
WAVELENGTHS IN LAYER = .714286
AT NOMINAL FREQUENCY = 50 MHZ
LAYER DELAY = 28.5714 NANOSEC

OUT/IN AMPLITUDE = .810101
RMS ENERGY LEVEL = .932112
PEAK FREQUENCY = 50 MHZ
SPECTRAL SKEWING = 0 %

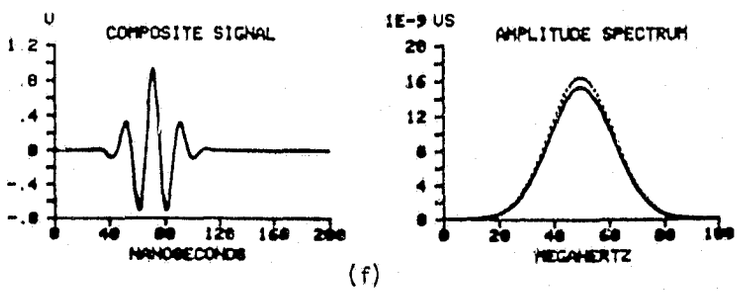

(f)

Figure 10. - Concluded.

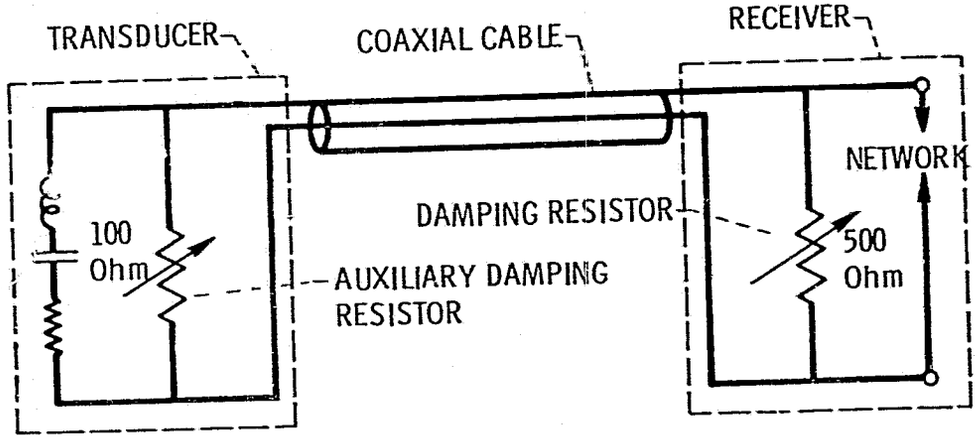

Figure 11. - Diagram showing auxiliary damping resistor included in ultrasonic transducer housing complementing damping resistor in receiver for improved impedance matching. (The piezoelement is represented by its equivalent reactive components in series, typical values are shown for damping resistors.)

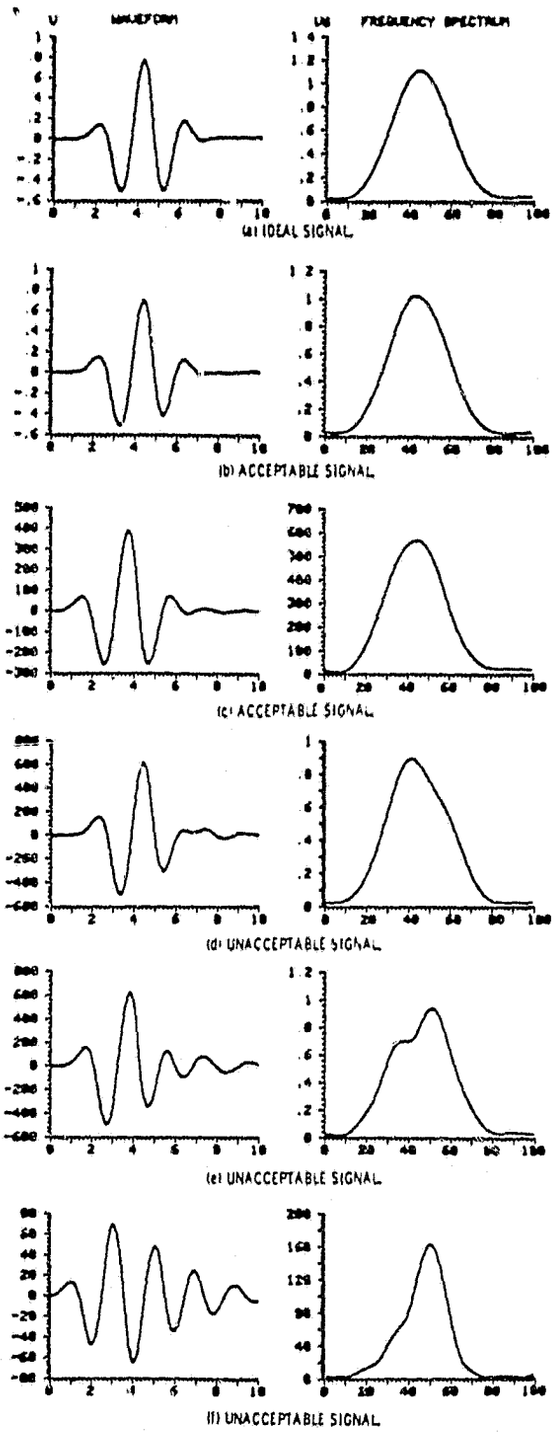

Figure 12. - Waveforms and frequency spectra associated with acceptable and unacceptable signals. Waveform series was generated by increasing electrical impedance mismatch of cable and transducer via the auxiliary damping resistor shown in Fig. 11. Auxiliary damping resistance increases from top to bottom, 2 to 50 Ohm, approximately.